Green Synthesis of Antimicrobial Silver Nanoparticles: Exploring Plant-Derived Reducing Agents from *Camellia Sinensis*, *Syzygium aromaticum*, and *Citrus Sinensis*

A. R. Sliem [1,*], S. Hassan [2,*], A. S. Shaban [2], and A. M Abdalla [2]

[1] *Technical research center (TRC), Nasr City, Cairo, Egypt.;*
[2] *Botany and Microbiology Department, Faculty of Science (Boys), Al-Azhar University, Cairo, Egypt*

[*] Corresponding author E-mail: ahmedragabtrcresearcher@gmail.com (A. R. Sliem)

ABSTRACT:

This study presents a comprehensive investigation into the green synthesis of silver nanoparticles (AgNPs) using botanical reducing agents derived from clove buds (CB), green tea leaves (GT), and orange peels (OP). The research highlights the significant influence of these botanical sources on the yield, stability, and nanoscale characteristics of the biosynthesized AgNPs (Bio-AgNPs). Notably, OP emerged as the most efficient reducing agent that produce AgNPs with the highest chemical yield (81%) and highest suspension stability (zeta potential of -72mV). While silver synthesis by CB extract (Ag-CB) demonstrated superior biocompatibility and lower cytotoxicity across multiple cell lines. The highest growth inhibition of Staphylococcus aureus was observed at 200 μg/mL for silver synthesis by OP extract (Ag-OP) with a zone of inhibition of 16.7 mm, surpassing the inhibition zones of 15.3 mm and 14.6 mm for silver synthesis by GT extract (Ag-GT) and Ag-CB, respectively. These findings underscore the potential of Ag-CB as a promising candidate for the synthesis of AgNPs, with implications for diverse biomedical applications. This research paves the way for future studies aimed at harnessing the versatility of botanical reducing agents, particularly Ag-CB, in the green synthesis of AgNPs and their potential applications in the biomedical and environmental fields. Further exploration of Ag-CB's potential beyond antimicrobial and cytotoxicity assessments is recommended. This study thus provides a significant contribution to the field of green nanotechnology, emphasizing the importance of selecting appropriate botanical reducing agents for the optimized synthesis of AgNPs.

Keywords: Botanical reducing agents; Silver nanoparticles (AgNPs); Clove buds; Green tea leaves; Orange peels; Antimicrobial activity; Cytotoxicity assessment.

INTRODUCTION

Nanomaterials, a dynamic domain within nanotechnology, hold the promise of reshaping nanoscale engineering (Baig et al., 2021, Patel and Pathak, 2021). and stand poised as pivotal components in the future technological landscape (ECHA, 2020, PNNL, 2021). Among these, metal nanoparticles (MNPs) are particularly noteworthy, demonstrating distinctive attributes and functionalities, especially in bio-related contexts (Wikipedia, 2024, Chandrakala et al., 2022). Noble metal nanoparticles (NMNPs), such as gold, silver, and platinum, exhibit remarkable physical, chemical, and optical properties that enable their use in various biomedical applications, such as antimicrobial, antioxidant, and cytotoxicity agents (Habibullah et al., 2021, Singh et al., 2021).

NMNPs, especially silver nanoparticles (AgNPs), exhibit a remarkable ability to bind to specific cells or tissues, presenting opportunities for microbial elimination (Lee et al., 2021, Chehelgerdi et al., 2023), cancer cell destruction, and diverse tissue treatments (Kaiser, 2021).

Within the subset of NMNPs, AgNPs are extensively researched due to their unique properties (Almatroudi, 2020), including a high surface-area-to-volume ratio, making them reactive and suitable for applications like drug delivery (Abdelmoneim et al., 2022), catalysis (Tarannum and Gautam, 2019), sensing (Chandra and Singh, 2018), antimicrobial (Patel and Pathak, 2021, Singh et al., 2015), and anticancer effects (Huq et al., 2022). Their easy functionalization further enhances their targeting capabilities (Galatage et al., 2021, Anandharamakrishnan and Anandharamakrishnan, 2014). Recent advancements at the intersection of biology and nanotechnology drive bio-nanotechnology (Joudeh and Linke, 2022), showcasing innovative methods for MNP synthesis and expanding their application range (Baig et al., 2021, Chiew et al., 2021, Fedlheim and Foss, 2001). A noteworthy breakthrough is the use of plant-based materials in MNP synthesis (Kohli, 2009, Liaqat et al., 2022).

An eco-friendly approach to the Bio-AgNPs involves utilizing plant extracts as reducing agents (Vanlalveni et al., 2021), tapping into the bioactive properties of various plants, such

as phytochemicals and enzymes (Asefian and Ghavam, 2024). This sustainable method not only presents a cost-effective alternative but also opens avenues for diverse applications (AlMasoud et al., 2021).

The green synthesis of AgNPs, employing plant extracts, is particularly valuable for applications involving interactions with living cells or tissues, given the biocompatibility and biodegradability of these materials (Liaqat et al., 2022).

In this study, we delve into the green synthesis of AgNPs by reducing silver ions (Ag^+) to silver atom (Ag) (Abdul Aziz et al., 2023). Three distinct plant extracts clove bud (CB), green tea (GT), and orange peel (OP) are employed as reducing agents (Danaei et al., 2021, Kaur and Kaushal, 2019). CB, belonging to the Myrtaceae family, utilizes eugenol as a potent reducing agent, with a weight percent of approximately 6 wt. % (Kalwar and Shan, 2018, Eng et al., 2018). GT, a member of the Theaceae family, relies on catechins, particularly EGCG, for reduction, with EGCG constituting 50-80 wt. % of the total catechin content (Widatalla et al., 2022, Dube et al., 2010). OP, from the Rutaceae family, utilizes citric acid as its primary reducing agent, with a weight percent of about 1.6 wt. % (Ramakuela et al., García-Merino et al., 2022, Sahay et al., 2023). However, the total weight percent of the reducing agents in dried orange peel powder was about 1.6 wt. % (Firdhouse and Lalitha, 2015, Harvey, 2021). In this work we tried to make our experiments environmentally friendly as possible as we can (Chemat et al., 2020). We have put some constraints to ensure our targets, such as using deionized water (DI) as the extraction medium of the reducing agents from the studied plant parts. However, water has variable extraction efficiency with the ingredients. Also, ambient conditions are used while extracting the reducing agents and in the reduction experiment of Ag^+. Characterization of the synthesized nanoparticles was conducted using FTIR, UV-vis. spectroscopy, XRD, TEM, and zetapotential analyzer. An investigation of the antimicrobial behaviors of the different synthesized AgNPs was performed against gram-positive bacteria (Bacillus subtilis and Staphylococcus aureus), gram-negative bacteria (Pseudomonas aeruginosa and Escherichia coli), and fungus (Candida albicans).

MATERIALS AND METHODS:

Chemicals and Reagents:

The dried leaves of GT were sourced from the commercial Cairo tea factory in Egypt. The dried buds of CB and fresh peels of OP were obtained from a local market. All chemicals, including silver nitrate ($AgNO_3$) and Sodium hydroxide (NaOH), were of research grade. Mueller Hinton Agar (MHA), and Muller Hinton Broth (MHB) were purchased. Sterile nutrient broth, McFarland No. 0.5 turbidity standard, 3-(4,5-Dimethylthiazol-2-yl)-2,5-diphenyltetrazolium bromide (MTT) for the MTT assay, Dulbecco's Modified Eagle Medium (DMEM), and Penicillin-streptomycin solution were sourced for cell culture. All solvents used were of analytical grade.

Preparation of Plant Samples:

The buds of CB, leaves of GT, and peels of OP were subjected to a detailed preparation process. Initially, these botanical materials were thoroughly rinsed with (DI) to remove any extraneous particles and debris. Following this, the cleaned plant specimens were dried in an oven at 60°C for a span of 12 h. This drying step ensured the complete removal of water molecules, thereby amplifying the concentration of bioactive components, including reducing agents, stabilizing agents, and capping agents. Post the drying process, the desiccated plant materials were carefully pulverized using a dedicated spice grinder. These powdered materials were weighed then securely packed into gauze bags. The use of gauze bags is a strategic and efficient step in the methodology. This practice not only simplifies the extraction process but also minimizes losses in the extract solution, eliminating the need for a filtration step. This optimized approach significantly reduces experimental time while preserving the integrity of the extracted components (Yeung et al., 2015).

Preparation of Aqueous Plant Extract Solutions:

The gauze bags, which were prepared in the previous step and contain powder of finely ground CB, GT, and OP, were submerged in 100 mL of (DI) in glass flasks to obtain 10% (m/v) aqueous extract solutions. These flasks were subjected to gentle shaking overnight under ambient conditions. The resulting aqueous solutions displayed distinct colors: dark brown for the CB extract, green for the GT extract, and orange for the OP extract. It is important to use these aqueous extracts

immediately after preparation to maintain their freshness, however, they can be stored at 4°C for up to one week, if necessary, to prevent microbial contamination. This step helps preserve the integrity of the extracts and ensures their suitability for subsequent procedures (Yeung et al., 2015).

Biosynthesis of Silver Nanoparticles (AgNPs):

The pH of the plant extract solutions was carefully adjusted to 10 using 1M sodium hydroxide (NaOH) aqueous solution (Anigol et al., 2023). Following this, each extract was slowly dropped to 150 mL of a 0.2 M silver nitrate aqueous solution ($AgNO_3$) under ambient conditions while stirring at 500 rpm on a magnetic stirrer. After the addition process was completed, the clear color of the $AgNO_3$ aqueous solution changed into a turbid reddish-brown colloid, labelled as Ag-CB, Ag-GT, and Ag-OP for the AgNPs prepared by using CB, GT, and OP extracted solutions, respectively. This visual change indicated the nucleation and growth of AgNPs (Yontar and Çevik, 2023).

Characterization Tools:

The plant extract solutions, both pre- and post-introduction of $AgNO_3$, underwent thorough characterization using diverse analytical techniques. Fourier Transform Infrared spectroscopy (FTIR, model: NICOLETi50) was used to analyze the functional groups present in the samples. The FTIR spectra were recorded at room temperature within the wavelength range of 400–4000 cm^{-1}, with 16 repeated scans. For the FTIR analysis, the liquid forms of the three extracts (GT, CB, and OP) were measured individually, while the synthesized colloids (Ag-CB, Ag-GT, and Ag-OP) were analyzed in their colloidal state. The absorbance and transmittance spectra of the AgNPs films in the wavelength range of 200-800 nm were captured using a UV-visible spectrophotometer (Perkin Elmer Lambda 35, Germany) at a scan speed of 300 nm min^{-1}. X-Ray Diffraction (XRD) analysis was conducted using a PANALYTICAL X'Pert Pro instrument equipped with a Siemens Smart CCD diffractometer. Monochromatized MoKα graphite radiation was operated at 40 kV and 30 mA with Cu Kα radiation source (λ = 1.5406 Å). The diffraction angles (2θ) ranged between 5 and 90. Morphological images of the samples were captured using high-resolution transmission electron microscopy (HR-TEM, Talose f200i Thermo Fisher Scientific). The colloids containing AgNPs (CB-Ag, GT-Ag, and OP-Ag) were deposited onto 200-mesh Cu grids coated with a carbon film. Bright-field imaging techniques were employed at 200 kV using a field emission gun electron source. The zeta potential, a crucial indicator of nanoparticle suspension stability, was measured using a HOREBA zeta potential analyser. The synthesized colloids were diluted with ethanol in a clear disposable zeta cell with graphite electrodes.

Evaluation of Antimicrobial activity:

Antimicrobial tests:

The antibacterial efficacy of the colloids containing AgNPs (Ag-CB, Ag-GT, and Ag-OP) was assessed using a disc diffusion method against gram-positive bacteria (Staphylococcus aureus (PTCC 1431), Bacillus subtilis (PTCC 1420)), Gram-negative bacteria (Escherichia coli (PTCC 1399), Pseudomonas aeruginosa (PTCC 1074)), and one pathogenic fungus (Candida albicans (PTCC 5027)) (Sameena and Thoppil, 2023). The microbial strains employed in this study were sourced from the Microbiology Laboratory, Botany and Microbiology Department, Al-Azhar University. The disc diffusion method is a widely adopted laboratory technique to determine the susceptibility of bacterial isolates to antimicrobials. In this method, discs impregnated with known concentrations of Ag-CB, Ag-GT, and Ag-OP were placed on agar plates that had been inoculated with a culture of the bacterium to be tested. The plates were incubated at 37°C for 18–24 hours (Zaidan et al., 2005). After diffusion, the concentration of the nanoparticle typically remains higher near the site of the nanoparticle disc but decreases with distance (Klančnik et al., 2010). The susceptibility of the bacteria to the specific nanoparticle was determined by measuring the zone of inhibition of bacterial growth around the disc (Atef et al., 2019). This method provides a visual representation of the antibacterial activity of the nanoparticles (Elisha et al., 2017).

Determination of cytotoxicity:

In 2012, there was work described a method for assessing the cytotoxicity of nanoparticles (NPs) by the MTT assay (Satyavani et al., 2012). In brief, Vero, HepG2, and MCF7 cells were seeded at a density of 1 × 105 cells/mL in a flat-bottomed 96-well microtiter plate (Kasvi-Brazil) and incubated for 24 hours at 37 °C, while the medium was supplemented with 10% heat-inactivated FBS (Invitrogen, USA), 2 mM L-glutamine (Merck, Germany), and 100

U/ml penicillin and 100 µg/ml streptomycin sulphate (Sigma-Aldrich, USA). Nanoparticles were prepared at concentrations ranging from 62.5 to 1000 µg/ml employing the cell culture medium DMEM and added to the plate in triplicate. After 72 hours, the treatments were removed and 100 µL of MTT reagent (0.5 mg/mL in DMEM) was added to each well and incubated for an additional 2 hours. The medium was then removed, and 100 µL of DMSO was added to the wells. The plate was read at 550 nm by a microplate reader to determine the half maximal cytotoxic concentration (IC_{50}). This method allows for the evaluation of the cytotoxicity of nanoparticles against a variety of cell lines.

RESULTS AND DISCUSSION:

Chemical yield of Bio-AgNPs:

Chemical yield refers to the amount of desired product obtained from a chemical reaction, usually expressed as a percentage of the theoretical maximum yield. It considers the efficiency of the reaction in producing the intended product (Wang et al., 2020, Abdelmoneim et al., 2022).

The actual produced silver powders were weighed and then compared them to their intended theoretical weights. The calculated chemical yields of the Bio-AgNPs by different reducing agents are assessed, revealing that the reduction capability by using 10%(w/v) OP exhibited the highest yield percentage (81%) compared to the yield percentage from CB (14%) and GT (12%). The high chemical yield of AgNPs obtained from the OP experiment may be attributed to the suitability of our designed environmentally friendly extraction route for the reducing agents existing in dried orange peel (Almatroudi, 2020). Alternatively, it may be due to the high reducing capability of citric acid in (OP) among eugenol in (CB) and EGCG in (GT) (Jadoun et al., 2021, Raj et al., 2022).

Chemical and material characterization of Bio-AgNPs:

FTIR analysis:

FTIR analysis was used to reveal the reducing, capping, and stabilizing roles of water-soluble biomolecules in the Bio-AgNPs using plant extracts. Figure 1(a) shows the FTIR spectra of CB, GT, and OP aqueous extracts, while Figure 1(b) displays their spectra after the formation of Bio-AgNPs. The investigation of the FTIR spectrum showed evidence for the reduction process of silver ion (Ag^+) to silver metal (Ag).

In the CB extract, eugenol was considered as the main ingredient of reduction capability. The peaks at 3456 ± 2 cm^{-1}, 2075 ± 2 cm-1 and 1641 ± 2 cm^{-1} indicate a broad O-H band, the presence of alkynes in the aqueous solution, and C=O stretching from eugenol carbonyl, respectively. A peak intensity decreases at 1641 cm^{-1} (eugenol carbonyl, C=O) after AgNPs production evidenced the mediated reduction. The alkyne peak at 2075 cm^{-1} was shifted slightly to higher wavenumber (2104 ± 2 cm^{-1}) after adding silver nitrate aqueous solution, confirm the formation of silver nanoparticles by a green synthesis method due to the help of alkynes as an intermediate state in the reaction between the aqueous solutions of plant extracts and silver nitrate aqueous solution at ambient conditions in an alkaline medium.

In the case of GT extract, catechins were the main reducing agents, and epigallocatechin gallate (EGCG) was the most dominant one in the catechin group that existed in green tea leaves. The FTIR spectrum confirmed the existence of four main peaks for EGCG, which were 3462 ± 2 cm^{-1}, 2100 ± 2 cm^{-1}, 1638 ± 2 cm^{-1}, and 1030 ± 2 cm^{-1}. The first peak indicates numerous hydroxyl groups present in the EGCG molecule, particularly those on the phenolic rings and the gallate moiety; The third peak corresponded to the carbonyl stretching of the B-ring in the flavonoid structure; and the final one represented aromatic C=C stretching in the EGCG molecule. After adding $AgNO_3$, peaks at 3462 ± 2 cm^{-1} and 1403 ± 2 cm^{-1} were noticed. They revealed a broad O-H band, which meant that hydroxyl groups were contributing to hydrogen bonding, confirming the capping and stabilizing of the synthesized AgNPs. However, as in the CB, a minor shifting with a decrease of intensity for COO^- stretching from carboxylate groups in organic acids and proteins (from 1638 cm^{-1} to 1641 cm^{-1}) indicated the reduction process. The alkaline peak was shifted slightly after adding silver nitrate aqueous solution as was happened in the CB sample, confirms the formation of AgNPs. indicating the formation of less complex, that the alkyne in GT is internal, meaning that it has no hydrogen atoms attached to the carbon atoms in the triple bond. The internal alkyne can form a silver diacetylide complex.

Citric acid was the main reducing agent found in OP. A peak at 3453 ± 2 cm^{-1} indicated

the O-H stretching vibration of the carboxylic acid groups and pectins resulted from citric acid and orange peel ingredients. A distinct peak at 1635 ± 2 cm^{-1} was assigned to the carbonyl stretching vibration of the carboxylic groups. The peak at 1397 ± 2 cm^{-1} correspond to the C-O stretching and bending vibrations of the carboxylic acid groups and the ester groups. This group played a crucial role in citric acid's antioxidant properties (reduction capability). However, the FTIR spectrum after the reaction showed possible contributions from proteins and amino acids (peak at 1121 ± 2 cm^{-1}), polysaccharides/glycosides (peak at 1116 ± 2 cm^{-1}), and pectins (broad O-H peak at 3453 ± 2 cm^{-1}) that suggested capping and stabilization. Finally, broad peaks at 672 ± 2 cm^{-1} (CB), 524 ± 2 cm^{-1} (GT), and 613 ± 2 cm^{-1} (OP) were found as shown in Figure 1(b). All these peaks corresponded to Ag-O stretching, confirming the presence of AgNPs.

The UV-Visible spectroscopy

The UV-Visible spectroscopy results suggested the optical properties of the silver nanoparticles. Figure 2 depicts the spectroscopic analysis that identified absorption peaks at 407 ± 2 nm, 444 ± 2 nm, and 456 ± 2 nm, corresponding to the reduction of silver nanoparticles using the aqueous extracts of CB, GT, and OP, respectively. The maximum wavelength (λmax) of 407, 444, and 456 nm indicated a strong absorption of light in the blue-green region of the spectrum by the silver nanoparticles (Quintero-Quiroz et al., 2019). This absorption phenomenon could be attributed to the interaction between the incident light and the oscillating free electrons present on the nanoparticle surface (Sahay et al., 2023). It is noteworthy that the λmax value could be influenced by several factors, including the size and shape of the nanoparticles, the concentration of the reducing agents, and the specific conditions under which the synthesis process occurred (Pauzi et al., 2023, Vanlalveni et al., 2021). Consequently, the observed λmax values implied that the plant-mediated synthesis of AgNPs used the reducing agents with optical properties that aligned with previous studies, indicating their successful formation (Marciniak et al., 2020, Jiang et al., 2010). This finding was consistent with the expected outcomes and validated the effectiveness of the plant-mediated synthesis approach.

The X-ray diffraction (XRD) analysis:

The XRD analysis is presented in Figure 3; the analysis of the three samples revealed distinct peaks at specific 2θ angles. These peaks existed in the three samples and corresponded to the diffraction of (111), (200), (220), (311), and (222) crystal planes in the face-centred-cubic silver (Dawadi et al., 2021). This pattern aligned with the standard Joint Committee on Powder Diffraction Standards (JCPDS) No. 04-0783 card for silver, confirming the successful synthesis of silver nanoparticles using the aforementioned reducing agents without any by-products.

Transmission Electron Microscopy (TEM):

The TEM analysis was conducted to investigate the nanoscale characteristics of the synthesized AgNPs using the extracts of botanical reducing agents from CB, GT, and OP. The TEM images provided insights into the morphology and size distribution of the AgNPs (Rautela and Rani, 2019). In Figure 4(a), the TEM analysis revealed the formation of spherical silver nanoparticles with an average size around 13.7 nm, 14.2 nm, and 7.2 nm, for centrifuged Ag-CB, Ag-GT, and Ag-OP, respectively. Uniform particle size distribution was observed in the Ag-CB and Ag-GT samples, with less distribution uniformity in the Ag-OP samples. Higher magnification images in Figure 4(b) gave some evidence about the formation of a very thin layer that covered the Bio-AgNPs for the three studied samples, which agreed with the previous FTIR analysis due to the presence of capping and stabilizing agents.

The zeta potential analysis:

The zeta potential values for the AgNPs prepared by using CB, GT, and OP extracted solutions were found to be -6.2 mV, -11.3 mV, and -72.5 mV, respectively. If the particles in suspension have a large negative or positive zeta potential, then they will tend to repel each other and there will be no tendency for the particles to come together (Vanlalveni et al., 2021). However, if the particles have a low zeta potential value, then there is no force to prevent the particles from coming together and flocculating (Sharma et al., 2016). The Ag-OP shows the highest negative zeta potential of -72.5 mV, indicating a high degree of suspension stability due to strong repulsive forces among the particles. On the other hand, the Ag-GT and Ag-CB had relatively low zeta potentials of -11.3 mV and -6.2 mV, respectively, suggesting a lower degree of stability in these suspensions. The nano-silver sample synthesized using OP extract (Ag-OP) had the lowest average particle size of 7.2 nm, with observation of many tiny particles around

5 nm in size from the TEM analysis. That may explain its higher zeta potential value (higher suspension stability) over the other two samples (Ag-CB and Ag-GT). These results suggest that the choice of botanical reducing agents can significantly influence the stability of the resulting AgNPs colloid (Vanlalveni et al., 2021).

Antimicrobial Studies:

Antimicrobial activity:

The antimicrobial activity of Bio-AgNPs derived from different plant parts, including leaves, buds, and peels, was assessed using the disc diffusion method against Gram-positive bacteria (Staphylococcus aureus (PTCC 1431), Bacillus subtilis (PTCC 1420)), Gram-negative bacteria (Escherichia coli (PTCC 1399), Pseudomonas aeruginosa (PTCC 1074)), and one pathogenic fungus (Candida albicans (PTCC 5027)) show in Figure 5. The botanical reducing agents utilized in this study were buds of Syzygium aromaticum (Ag-CB), leaves of Camelilia Sinensis (Ag-GT), and peels of Citrus Sinensis (Ag-OP) extracts. The disc diffusion method was employed to evaluate the antimicrobial activity of these nanoparticles at varying concentrations (12.5 μg/mL, 25 μg/mL, 50 μg/mL, 100 μg/mL, and 200 μg/mL), as shown in Figure 6. In the concentration range of 50-200 μg/mL, Ag-OP exhibited significantly higher microbial growth inhibition compared to Ag-GT and Ag-CB. For example, at 100 μg/mL, the growth inhibition zones for Bacillus subtilis were 12.3, 12.0, and 13.6 mm for Ag-CB, Ag-GT, and Ag-OP, respectively, in comparison to the 13.3 mm caused by AgNPs at the same concentration. At 200 μg/mL, growth inhibition zones for Ag-OP were significantly higher than those recorded for Ag-GT and Ag-CB. The highest growth inhibition of Staphylococcus aureus was observed at 200 μg/mL of Ag-OP with a zone of inhibition of 16.7 mm, surpassing the inhibition zones of 15.3 mm and 14.6 mm for Ag-GT and Ag-CB, respectively.

Furthermore, the growth inhibition of Pseudomonas aeruginosa at 100 and 200 μg/mL of Ag-OP was significantly higher compared to Ag-GT and Ag-CB. However, there was no significant difference in growth inhibition between standard AgNPs and Ag-OP against Pseudomonas aeruginosa. Interestingly, no activity was observed at 25 μg/mL of standard AgNPs against Escherichia coli, but at 200 μg/mL, Ag-OP caused significantly higher inhibition compared to other Bio-AgNPs treatments, achieving maximum growth inhibition with zones of 17.6 mm and 17.3 mm for standard AgNPs and Bio-AgNPs.

Data analysis revealed significant differences in inhibition caused by Bio-AgNPs using OP and CB against Candida albicans compared to Bio-AgNPs using GT at 200 μg/mL. The highest inhibition of Candida albicans (15.3 mm) was recorded at 200 μg/mL of Bio-AgNPs using OP. The results are summarized in Figure 5. According to (Thenmozhi et al., 2013), the growth of pathogenic bacteria and fungi was hindered by Bio-AgNPs. Various pieces of evidence elucidate the antifungal mechanisms of Ag-NPs, such as the release of free silver ions, the generation of free radicals that disrupt membrane lipids and functions, and the creation of pits in the cell wall due to the binding of Ag-NPs to external proteins (Danilczuk et al., 2006).

Cytotoxicity Assessment:

At 1000 μg/ml, Ag-GT exhibited the highest toxicity (90%), followed by Ag-OP (71%) and Ag-CB (77%) as shown in Figure 7. Ag-CB demonstrated lower toxicity across concentrations, with higher viability percentages compared to Ag-GT and Ag-OP. The IC_{50} values indicate that Ag-GT has a higher inhibitory concentration than Ag-CB and Ag-OP, suggesting that Ag-GT may be less toxic. These findings are consistent with previous studies that have reported the toxicity of Ag-GT and Ag-CB. The results of this study suggest that CB extract solution may be a promising reducing agent for synthesizing AgNPs with biomedical applications potential for Vero cells. Further research is needed to explore the potential of CB as a reducing agent for other applications. The results of this study demonstrate that effect of AgNPs biosynthesized by using GT, OP, and CB extracts solutions exhibit varying degrees of toxicity. Ag-GT was found to be the most toxic, followed by Ag-OP and Ag-CB suspension solutions. CB suspended solution consistently exhibited lower toxicity across concentrations, indicating better viability compared to Ag-GT and Ag-OP suspended solutions. The IC_{50} values reinforce Ag-CB suspended solution as a more effective reducing agent in HepG2 cells, requiring lower concentrations for half-maximal inhibition. These findings are consistent with previous studies that have reported the toxicity of Ag-GT and Ag-CB suspended solutions.

At 1000 µg/ml, Ag-GT exhibited the highest toxicity (96%), followed by Ag-OP (71%) and Ag-CB (77%) as shown in Figure 8. Ag-CB consistently exhibited lower toxicity across concentrations, indicating better viability compared to Ag-GT and Ag-OP. The IC_{50} values reinforce Ag-CB suspended solution as a more effective in HepG2 cells, requiring lower concentrations for half-maximal inhibition.

The results of this study suggest that CB extract solution may be a promising reducing agent for Bio-AgNPs with lower cytotoxicity in HepG2 cells, suggesting its potential for biomedical applications. Further research is needed to explore the potential of CB extract solution as a reducing agent for other applications.

At 1000 µg/ml, Ag-GT exhibited the highest toxicity (79%), followed by Ag-OP (71%) and Ag-CB (77%) as shown in Figure 9. Ag-CB consistently showed lower toxicity across concentrations, indicating better viability compared to Ag-GT and Ag-OP. The IC_{50} values reinforce Ag-CB as a more effective suspension solution against Mcf7 cells, requiring lower concentrations for half-maximal inhibition.

The results of this study demonstrate that Ag-GT, Ag-OP, and Ag-CB exhibit varying degrees of toxicity. Ag-GT was found to be the most toxic, followed by Ag-OP and Ag-CB. Ag-CB suspended solution consistently showed lower toxicity across concentrations, indicating better viability compared to Ag-GT and Ag-OP extract solutions. The IC_{50} values reinforce Ag-CB suspended solution as a more effective suspension solution against Mcf7 cells, requiring lower concentrations for half-maximal inhibition. These findings are consistent with previous studies that have reported the toxicity of Ag-GT and Ag-CB suspension solutions.

CONCLUSION:

This study investigates the synthesis and characterization of silver nanoparticles (AgNPs) utilizing botanical reducing agents derived from clove buds (CB), green tea leaves (GT), and orange peels (OP). The chemical yield assessment, representing reaction efficiency, reveals that employing 10% (w/v) OP as a reducing agent yields the highest AgNPs percentage (81%), surpassing CB (14%) and GT (12%). The environmentally friendly extraction route and the high reducing capability of citric acid in OP contribute to its superior yield. Material characterization encompasses Fourier-transform infrared (FTIR) analysis, UV-Visible spectroscopy, X-ray diffraction (XRD), transmission electron microscopy (TEM), and zeta potential analysis. FTIR spectra elucidate the roles of water-soluble biomolecules in AgNP reduction, capping, and stabilization. UV-Visible spectroscopy identifies absorption peaks at 407 nm (CB), 444 nm (GT), and 456 nm (OP), indicating successful AgNP formation. XRD analysis confirms the face-centered-cubic silver crystal structure without by-products. TEM analysis reveals spherical AgNPs with varying average sizes (CB: 13.7 nm, GT: 14.2 nm, OP: 7.2 nm), and zeta potential values indicate high suspension stability for Ag-OP (-72.5 mV) compared to Ag-GT (-11.3 mV) and Ag-CB (-6.2 mV). Furthermore, antimicrobial assessments against various microorganisms highlight Ag-OP superior properties in the concentration range of 50-200 µg/mL compared to Ag-GT and Ag-CB. Cytotoxicity evaluations using Vero, HepG2, and Mcf7 cell lines reveal varying toxicity levels among the reducing agents, with clove consistently exhibiting lower toxicity and higher efficacy, particularly in HepG2 cells. In conclusion, this research emphasizes the significant influence of botanical reducing agents on the chemical yield, stability, and nanoscale characteristics of biosynthesized AgNPs. The findings contribute valuable insights for potential biomedical and environmental applications of these green-synthesized nanoparticles. Further exploration of clove's versatility for various applications beyond antimicrobial and cytotoxicity assessments is recommended.

REFERENCES

Abdelmoneim, H.M., Taha, T.H., Elnouby, M.S., Abushady, H.M. 2022: Extracellular biosynthesis, OVAT/statistical optimization, and characterization of silver nanoparticles (AgNPs) using Leclercia adecarboxylata THHM and its antimicrobial activity. *Microbial Cell Factories,* 21**:** 277 .

Abdul Aziz, A.H., Rizkiyah, D.N., Qomariyah, L., Irianto, I., Che Yunus, M.A., Putra, N.R. 2023: Unlocking the Full Potential of Clove (Syzygium aromaticum) Spice: An Overview of Extraction Techniques, Bioactivity, and Future Opportunities in the Food and Beverage Industry. *Processes,* 11**:** 2453 .

Almasoud, N., Alhaik, H., Almutairi, M., Houjak, A., Hazazi, K., Alhayek, F., Aljanoubi, S., Alkhaibari, A., Alghamdi, A., Soliman, D.A. 2021: Green nanotechnology synthesized silver nanoparticles: Characterization and testing its

antibacterial activity. *Green Processing and Synthesis,* 10**:** 518-528 .

Almatroudi, A. 2020: Silver nanoparticles: Synthesis, characterisation and biomedical applications. *Open life sciences,* 15**:** 819 .839-

Anandharamakrishnan, C., Anandharamakrishnan, C. 2014: Characterization of Nanoparticles. *Techniques for Nanoencapsulation of Food Ingredients***:** 65-67 .

Anigol, L.B., Sajjan, V.P., Gurubasavaraj, P.M., Ganachari, S.V., Patil, D. 2023: Study on the effect of pH on the biosynthesis of silver nanoparticles using Capparis moonii fruit extract: their applications in anticancer activity, biocompatibility and photocatalytic degradation. *Chemical Papers,* 77**:** 3327-3345 .

Asefian, S., Ghavam, M. 2024: Green and environmentally friendly synthesis of silver nanoparticles with antibacterial properties from some medicinal plants. *BMC biotechnology,* 24**:** 5 .

Atef, N.M., Shanab, S.M., Negm, S.I., Abbas, Y.A. 2019: Evaluation of antimicrobial activity of some plant extracts against antibiotic susceptible and resistant bacterial strains causing wound infection. *Bulletin of the National Research Centre,* 43**:** 1-11 .

Baig, N., Kammakakam, I., Falath, W. 2021: Nanomaterials: A review of synthesis methods, properties, recent progress, and challenges. *Materials Advances,* 2**:** 1821-1871 .

Chandra, A., Singh, M. 2018: Biosynthesis of amino acid functionalized silver nanoparticles for potential catalytic and oxygen sensing applications. *Inorganic Chemistry Frontiers,* 5**:** 233-257 .

Chandrakala, V., Aruna, V., Angajala, G. 2022: Review on metal nanoparticles as nanocarriers: Current challenges and perspectives in drug delivery systems. *Emergent Materials,* 5**:** 1593-1615 .

Chehelgerdi, M., Chehelgerdi, M., Allela, O.Q.B., Pecho, R.D.C., Jayasankar, N., Rao, D.P., Thamaraikani, T., Vasanthan, M., Viktor, P., Lakshmaiya, N. 2023: Progressing nanotechnology to improve targeted cancer treatment: overcoming hurdles in its clinical implementation. *Molecular cancer,* 22 .169 :

Chemat, F., Vian, M.A., Fabiano-Tixier, A.S., Nutrizio, M., Jambrak, A.R., Munekata, P.E., Lorenzo, J.M., Barba, F.J., Binello, A., Cravotto, G. 2020: A review of sustainable and intensified techniques for extraction of food and natural products. *Green Chemistry,* 22**:** 2325-2353 .

Chiew, C., Morris, M.J., Malakooti, M.H. 2021: Functional liquid metal nanoparticles: synthesis and applications. *Materials Advances,* 2**:** 7799-7819 .

Danaei, M., Motaghi, M.M., Naghmachi, M., Amirmahani, F., Moravej, R. 2021: Green synthesis of silver nanoparticles (AgNPs) by filamentous algae extract: Comprehensive evaluation of antimicrobial and anti-biofilm effects against nosocomial pathogens. *Biologia,* 76**:** 3057-3069 .

Danilczuk, M., Lund, A., Sadlo, J., Yamada, H., Michalik, J. 2006: Conduction electron spin resonance of small silver particles. *Spectrochimica Acta Part A: Molecular and Biomolecular Spectroscopy,* 63**:** 189-191 .

Dawadi, S., Katuwal, S., Gupta, A., Lamichhane, U., Thapa, R., Jaisi, S., Lamichhane, G., Bhattarai, D.P., Parajuli, N. 2021: Current research on silver nanoparticles: synthesis, characterization, and applications. *Journal of nanomaterials,* 2021**:** 1-23 .

Dube, A., Ng, K., Nicolazzo, J.A., Larson, I. 2010: Effective use of reducing agents and nanoparticle encapsulation in stabilizing catechins in alkaline solution. *Food chemistry,* 122**:** 662-667 .

Echa, E.C.A. 2020: Nanomaterials. ECHA, EUROPEAN CHEMICALS AGENCY.

Elisha, I.L., Botha, F.S., Mcgaw, L.J., Eloff, J.N. 2017: The antibacterial activity of extracts of nine plant species with good activity against Escherichia coli against five other bacteria and cytotoxicity of extracts. *BMC complementary and alternative medicine,* 17**:** 1-10 .

Eng, Q.Y., Thanikachalam, P.V., Ramamurthy, S. 2018: Molecular understanding of Epigallocatechin gallate (EGCG) in cardiovascular and metabolic diseases. *Journal of ethnopharmacology,* 210**:** 296-310 .

Fedlheim, D.L., Foss, C.A. 2001: *Metal nanoparticles: synthesis, characterization, and applications*: CRC press.

Firdhouse, M.J., Lalitha, P. 2015: Biosynthesis of silver nanoparticles and its applications. *Journal of Nanotechnology,* 2015 .

Galatage, S.T., Hebalkar, A.S., Dhobale, S.V., Mali, O.R., Kumbhar, P.S., Nikade, S.V., Killedar, S.G. 2021: Silver nanoparticles: properties, synthesis, characterization, applications and future trends. *Silver Micro-Nanoparticles Prop Synth Charact Appl* .

García-Merino, B., Bringas, E., Ortiz, I. 2022: Synthesis and applications of surface-modified magnetic nanoparticles: Progress and future prospects. *Reviews in Chemical Engineering,* 38**:** 821-842 .

Habibullah, G., Viktorova, J., Ruml, T. 2021: C urrent strategies for noble metal nanoparticle synthesis. *Nanoscale Research Letters,* 16**:** 1-12 .

Harvey, D. 2021: Analytical chemistry 2.1 (Open access; CC-BY-VC-SA 4.0).

Huq, M.A., Ashrafudoulla, M., Rahman, M.M., Balusamy, S.R., Akter, S. 2022: Green synthesis and potential antibacterial applications of bioactive silver nanoparticles: A review. *Polymers,* 14**:** 742 .

Jadoun, S., Arif, R., Jangid, N.K., Meena, R.K. 2021: Green synthesis of nanoparticles using plant extracts: A review. *Environmental Chemistry Letters,* 19**:** 355-374 .

Jiang, X., Chen, C., Chen, W., Yu, A. 2010: Role of citric acid in the formation of silver nanoplates through a synergistic reduction approach. *Langmuir,* 26**:** 4400-4408 .

Joudeh, N., Linke, D. 2022: Nanoparticle classification, physicochemical properties, characterization, and applications: a comprehensive review for biologists. *Journal of Nanobiotechnology,* 20**:** 262 .

Kaiser, G.E. 2021: My First 51 Years Teaching Microbiology at The Community College of Baltimore County. *Teaching and Learning Excellence through Scholarship,* 1 .

Kalwar, K., Shan, D. 2018: Antimicrobial effect of silver nanoparticles (AgNPs) and their mechanism–a mini review. *Micro & Nano Letters,* 13**:** 277-280 .

Kaur, K., Kaushal, S. 2019: Phytochemistry and pharmacological aspects of Syzygium aromaticum: A review. *Journal of Pharmacognosy and Phytochemistry,* 8**:** 398-406 .

Klančnik, A., Piskernik, S., Jeršek, B., Možina, S.S. 2010: Evaluation of diffusion and dilution methods to determine the antibacterial activity of plant extracts. *Journal of microbiological methods,* 81**:** 121-126 .

Kohli, R. 2009: The Nature and Characterization of Nanoparticles. *MRS Online Proceedings Library (OPL),* 1184**:** 1184-HH04-01 .

Lee, N.K., Kim, S.N., Park, C.G. 2021: Immune cell targeting nanoparticles: a review. *Biomaterials Research,* 25**:** 1-11 .

Liaqat, N., Jahan, N., Anwar, T., Qureshi, H. 2022: Green synthesized silver nanoparticles: Optimization, characterization, antimicrobial activity, and cytotoxicity study by hemolysis assay. *Frontiers in Chemistry,* 10**:** 952006 .

Marciniak, L., Nowak, M., Trojanowska, A., Tylkowski, B., Jastrzab, R. 2020: The effect of pH on the size of silver nanoparticles obtained in the reduction reaction with citric and malic acids. *Materials,* 13**:** 5444 .

Patel, J.K., Pathak, Y.V. 2021: *Emerging technologies for nanoparticle manufacturing*: Springer.

Pauzi, N., Mohamad, S., Ghazali, S., Jamari, S.S. 2023: Evaluation of Glucose Reduction for Silver Nanoparticles Synthesis with Nanocrystalline Cellulose Matrix. *BioNanoScience,* 13**:** 1695-1702 .

Pnnl, P.N.N.L. 2021: Nanomaterials .PNNL, Pacific Northwest National Laboratory.

Quintero-Quiroz, C., Acevedo, N., Zapata-Giraldo, J., Botero, L.E., Quintero, J., Zárate-Triviño, D., Saldarriaga, J., Pérez, V.Z. 2019: Optimization of silver nanoparticle synthesis by chemical reduction and evaluation of its antimicrobial and toxic activity. *Biomaterials research,* 23**:** 27 .

Raj, B., John, S., Chandrakala, V., Kumari, G.H. 2022: Green Extraction Techniques for Phytoconstituents from Natural Products. *Medicinal Plants.* IntechOpen.

Ramakuela, M., Adeniyi, A., Onyango, M., Mbaya, R., Oyewo, O.A. Performance Evaluation of Orange Peels as Anti-Scaling Agent for Pretreatment of Water .

Rautela, A., Rani, J. 2019: Green synthesis of silver nanoparticles from Tectona grandis seeds extract: characterization and mechanism of antimicrobial action on different microorganisms. *Journal of Analytical Science and Technology,* 10**:** 1-10 .

Sahay, A., Tomar, R.S., Shrivastava, V., Chauhan, P.S. 2023: Eugenol Loaded Ag-Ti-Co Nanocomposite as a Promising Antimicrobial and Antioxidative Agent. *BioNanoScience,* 13**:** 339-351 .

Sameena, V., Thoppil, J. 2023: In vitro antibacterial efficacy of methanolic plant extract and biosynthesized silver nanoparticles from Euphorbia species against two selected foodborne pathogens. *Nanotechnology for Environmental Engineering***:** 1-13 .

Satyavani, K., Gurudeeban, S., Ramanathan, T., Balasubramanian, T. 2012: Toxicity study of silver nanoparticles synthesized from Suaeda monoica on Hep-2 cell line. *Avicenna journal of medical biotechnology,* 4**:** 35 .

Sharma, V., Tarachand, T., Ganesan, V., Okram, G.S. 2016: Zeta-potential and particle size studies of silver sulphide nanoparticles. *AIP Conference Proceedings.* AIP Publishing.

Singh, H., Bamrah, A., Bhardwaj, S.K., Deep, A., Khatri, M., Brown, R.J., Bhardwaj, N., Kim, K.H. 2021: Recent advances in the application of noble metal nanoparticles in colorimetric sensors for lead ions. *Environmental Science: Nano,* 8**:** 863-889 .

Singh, R., Shedbalkar, U.U., Wadhwani, S.A., Chopade, B.A. 2015: Bacteriagenic silver nanoparticles: synthesis, mechanism, and applications. *Applied microbiology and biotechnology,* 99**:** 4579-4593 .

Tarannum, N., Gautam, Y.K. 2019: Facile green synthesis and applications of silver nanoparticles: a state-of-the-art review. *RSC advances,* 9**:** 34926-34948 .

Thenmozhi, M., Kannabiran, K., Kumar, R., Khanna, V.G. 2013: Antifungal activity of Streptomyces sp. VITSTK7 and its synthesized Ag2O/Ag nanoparticles against medically important Aspergillus pathogens. *Journal de mycologie médicale,* 23**:** 97-103 .

Vanlalveni, C., Lallianrawna, S., Biswas, A., Selvaraj, M., Changmai, B., Rokhum, S.L. 2021: Green synthesis of silver nanoparticles using plant extracts and their antimicrobial activities: A review of recent literature. *RSC advances,* 11**:** 2804-2837 .

Wang, Y., Wei, S., Wang, K., Wang, Z., Duan, J., Cui, L., Zheng, H., Wang, Y., Wang, S. 2020: Evaluation of biosynthesis parameters, stability and biological activities of silver nanoparticles synthesized by Cornus Officinalis extract under 365 nm UV radiation. *RSC advances,* 10**:** 27173-27182 .

Widatalla, H.A., Yassin, L.F., Alrasheid, A.A., Ahmed, S.A.R., Widdatallah, M.O., Eltilib, S.H., Mohamed, A.A. 2022: Green synthesis of silver nanoparticles using green tea leaf extract, characterization and evaluation of antimicrobial activity. *Nanoscale Advances,* 4**:** 911-915 .

Wikipedia, T.F.E. 2024: Nanoparticle. Wikipedia.

Yeung, E.C.T., Stasolla, C., Sumner, M.J., Huang, B.Q. 2015: Plant microtechniques and protocols. Springer.

Yontar, A.K., Çevik, S. 2023: Effects of Plant Extracts and Green-Synthesized Silver Nanoparticles on the Polyvinyl Alcohol (PVA) Nanocomposite Films. *Arabian Journal for Science and Engineering***:** 1-18 .

Zaidan, M., Noor Rain, A., Badrul, A., Adlin, A., Norazah, A., Zakiah, I. 2005: In vitro screening of five local medicinal plants for antibacterial activity using disc diffusion method. *Trop biomed,* 22**:** 165-170 .

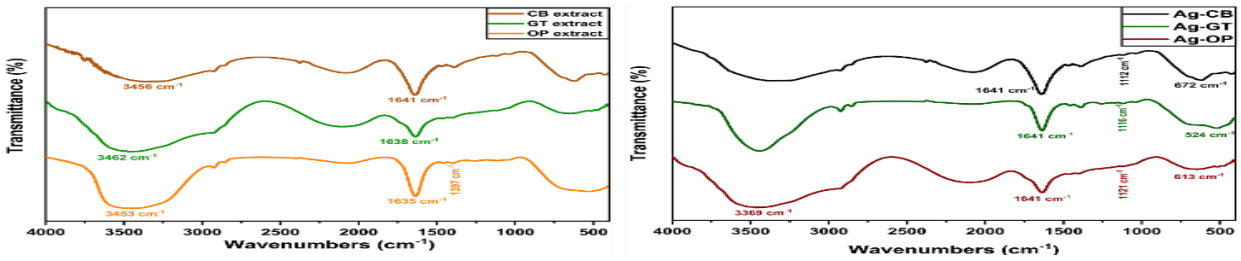

Figure 1:(a) CB, GT, and OP extracts FTIR spectra, and (b) Biosynthesis Ag-CB, Ag-GT, and Ag-OP

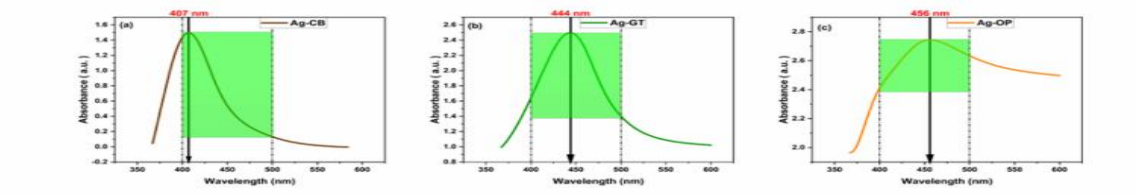

Figure 2: UV-visible spectrum of Bio-AgNPs synthesized using different plant extracts: (a) Eugenol from dried CB, EGCG from dried GT, and Citric acid from dried OP.

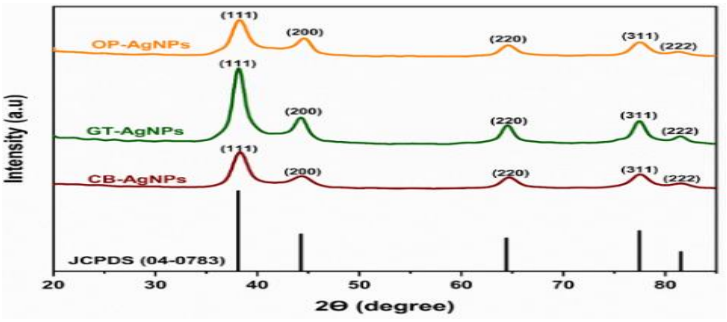

Figure 3: XRD diagram for Bio-AgNPs synthesized using different plant extracts from dried CB, dried GT, and dried OP.

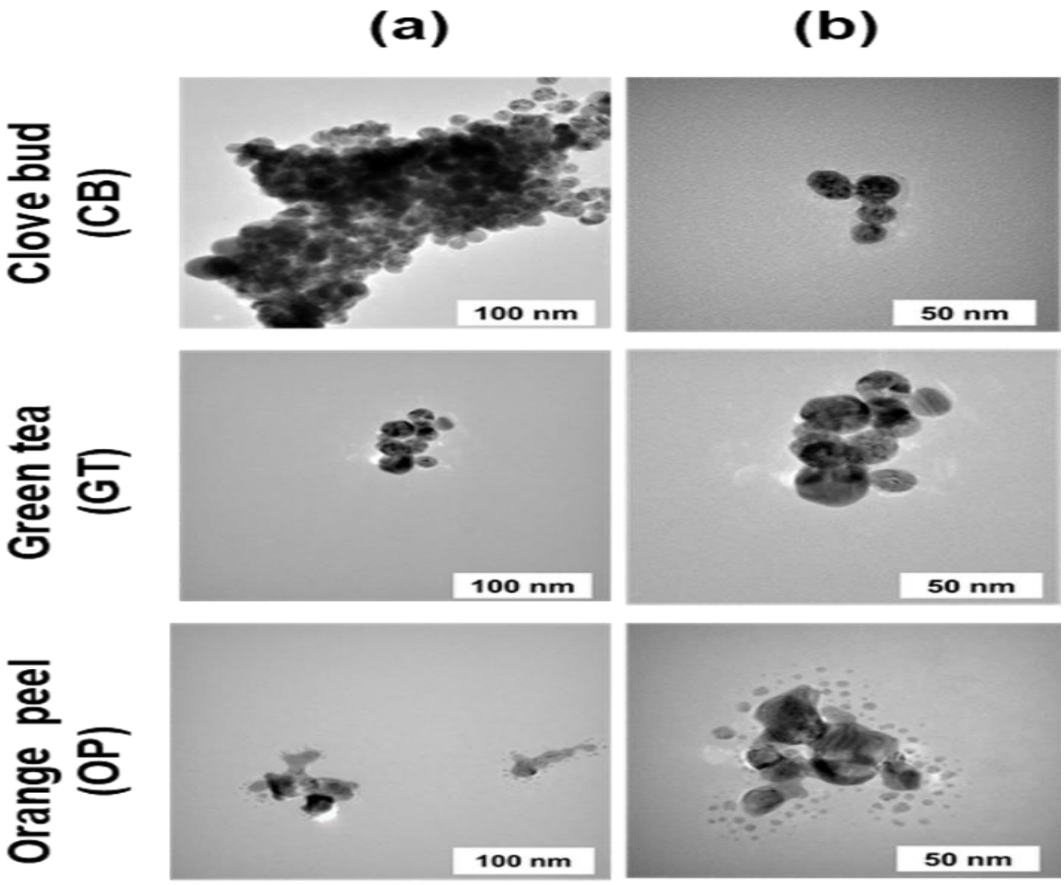

Figure 4: TEM analysis for Bio-AgNPs by using CB, GT, and OP extract solution. (a) magnification at 200 kx, and (b) magnification at 400 kx.

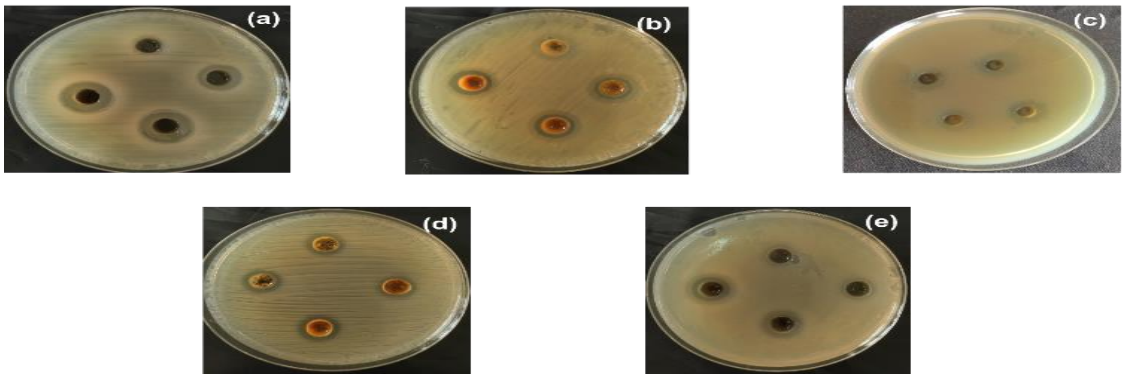

Figure 5: Antimicrobial activity of Bio-AgNPs at a concentration of 1000 µg/mL against human pathogenic microbes. a: Staphylococcus aureus PTCC 1431, b: Bacillus subtilis PTCC 1420, c: Escherichia coli PTCC 1399, d: Pseudomonas aeruginosa PTCC 1074, and e: Candida albicans PTCC 5027

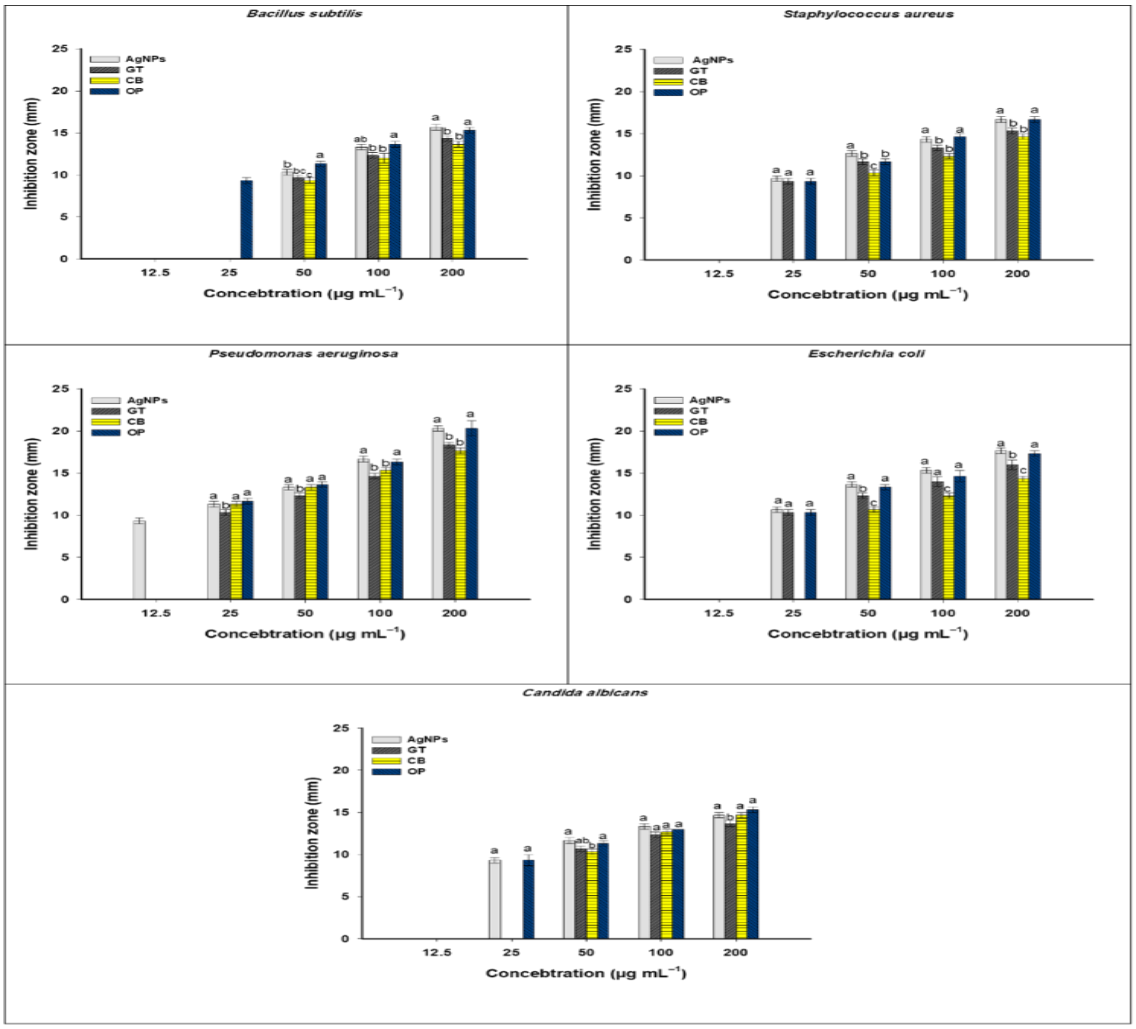

Figure 6: Variation of zone of inhibition against different pathogenic microorganisms at different concentrations of Bio-AgNPs

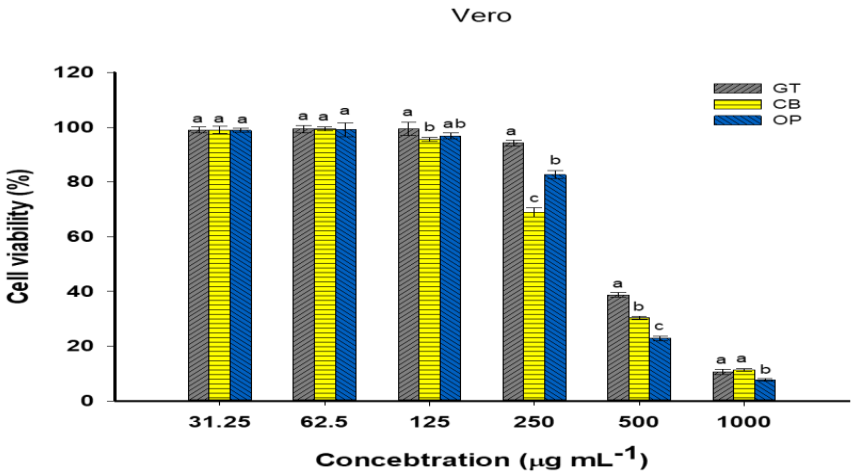

Figure 7: Cytotoxicity Assessment by using different concentrations from Bio-AgNPs against Vero Cell Line

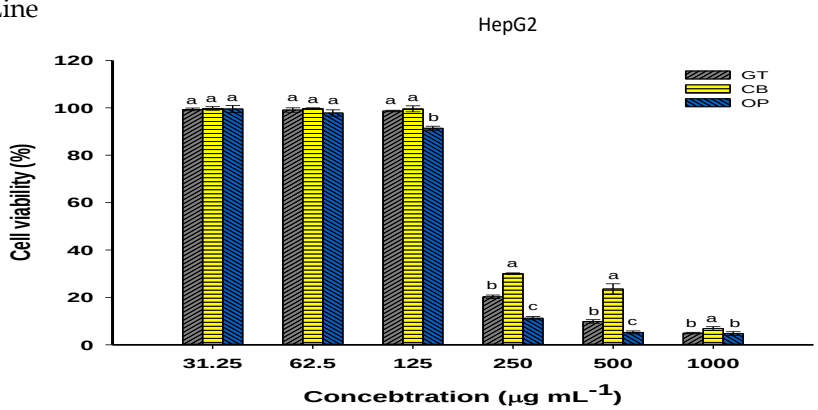

Figure 8: Cytotoxicity Assessment by using different concentrations from Bio-AgNPs against HepG2 Cell Line

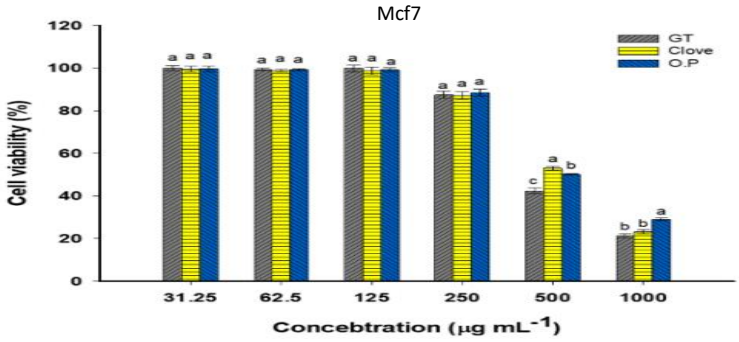

Figure 9: Cytotoxicity Assessment by using different concentrations from Bio-AgNPs against Mcf7 Cell Line

التحضير الأخضر لجسيمات الفضة النانومترية المضادة للميكروبات: إستكشاف عوامل الإختزال المستمدة من براعم القرنفل، أوراق نبات الشاي الأخضر، قشور البرتقال

أحمد رجب سليم [1,*], سعد الدين حسين عفيفي [2], عباس أحمد الغمري [2], عبدالغني صبحي شعبان [2], أحمد محمد عبدالله [2]

[1] *مركز البحوث الفنية، مدينة نصر، القاهرة ،مصر.*

[2] *قسم النبات والميكروبيولوجي، كلية العلوم (بنين)، جامعة الأزهر، مدينة نصر، القاهرة، مصر.*

[*] البريد الإلكتروني للباحث الرئيسي: ahmedragabtrcresearcher@gmail.com

الملخص

تقديم تحقيق شامل في تخليق جسيمات الفضة النانومترية باستخدام عوامل الاختزال النباتية المستمدة من مستخلصات براعم القرنفل، وأوراق نبات الشاي الأخضر، وقشور البرتقالب). يسلط البحث الضوء على التأثير البارز لهذه المصادر النباتية على كمية النسبة التي يتم تحضيرها من الفضة النانومترية وعلى إستقرار وخصائص المواد النانومترية لجسيمات الفضة النانومترية المختلفة المختزلة حيوياً. وقد تبين بشكل ملحوظ أن قشر البرتقال يظهر كعامل اختزال فعال يُنتج جسيمات الفضة النانومترية بأعلى نسبة إنتاج كيميائي (81%) وأعلى استقرار للمواد المعلقة (قدرة- زيتا= -72ملي فولت). في حين أظهرت جسيمات الفضة النانومترية التي تم تحضيرها بإستخدام عوامل الإختزال الموجودة في براعم القرنفل توافقاً حيوياً متفوقاً وسمية خلوية أقل خلال إختبارهاعبر خطوط خلايا متعددة. تؤكد هذه النتائج إمكانيات الفضة المنتجة بواسطة مستخلص براعم القرنفل كعامل إختزال ممتاز لتحضير جسيمات الفضة النانومترية ، مما يعزز تطلعاتها في مجالات التطبيقات الطبية المتنوعة. ويمهد هذا البحث الطريق لدراسات مستقبلية تهدف إلى استغلال تنوع عوامل الإختزال النباتية، وبشكل خاص المنتجة بواسطة مستخلص براعم القرنفل ، في تحضير جسيمات الفضة النانومترية بطريقة خضراء وإستكشاف تطبيقاتها المحتملة في الميدانين الطبي والبيئي. ويُفضل مواصلة استكشاف إمكانيات أكثر للفضة المنتجة عن طريق إستخدام مستخلص براعم القرنفل كونها تستخدم كمضادات أحيائية و لها فاعلية ملحوظة في إختبارات السمية الخلوية. تقدم هذه الدراسة إسهامًا كبيرًا في ميدان التكنولوجيا النانوية الخضراء، مؤكدة على أهمية إختيار عوامل الإختزال النباتية المناسبة لتحقيق تخليق محسن لجسيمات الفضة النانومترية.

الكلمات الاسترشادية: مواد إختزالية نباتية, الجسيمات النانوية الفضية, براعم القرنفل, أوراق الشاي الأخضر, قشور البرتقال, النشاط الضد ميكروبي, التقييم المضاد للسمية.